Reprinted from

JOURNAL OF THE PHYSICAL SOCIETY OF JAPAN

LETTER

Thickness Dependence of Surface Structure and Superconductivity in Pb Atomic Layers

Haruko Toyama, Hongrui Huang, Tomonori Nakamura, Leonid V. Bondarenko, Alexandra Y. Tupchaya, Dimitry V. Gruznev, Akari Takayama, Andrey V. Zotov, Alexander A. Saranin, and Shuji Hasegawa

J. Phys. Soc. Jpn. **87**, 113601 (2018)

Journal of the Physical Society of Japan **87**, 113601 (2018) **Letters**
https://doi.org/10.7566/JPSJ.87.113601

Thickness Dependence of Surface Structure and Superconductivity in Pb Atomic Layers

Haruko Toyama[1*], Hongrui Huang[1], Tomonori Nakamura[1], Leonid V. Bondarenko[2], Alexandra Y. Tupchaya[2], Dimitry V. Gruznev[2], Akari Takayama[1], Andrey V. Zotov[2,3], Alexander A. Saranin[2,3], and Shuji Hasegawa[1]

[1]*Department of Physics, University of Tokyo, Bunkyo, Tokyo 113-0033, Japan*
[2]*Institute of Automation and Control Processes, 690041, Vladivostok, Russia*
[3]*School of Natural Science, Far Eastern Federal University, 690950, Vladivostok, Russia*

(Received May 8, 2018; accepted September 27, 2018; published online October 25, 2018)

Two-dimensional superconductivity in atomic layers has recently attracted considerable attention owing to its intriguing different physical properties compared to that of the three-dimensional cases. By using an in situ four-point probe method in ultrahigh vacuum, we measured the transport properties of Pb atomic layers with different thicknesses and structures grown on a Ge(111) substrate at low temperature. The transition to zero resistance was observed around 4 and 6 K for deposition amounts of Pb corresponding to 3 and 10 monolayers, respectively. We found that both samples are two-dimensional superconductors because the coherence length is much longer than the film thickness. We also found that even though the surface is not entirely covered by Pb(111) islands, the samples exhibit superconductivity which indicates that superconductivity is induced in the wetting layer by the proximity effect from the Pb islands. For understanding two-dimensional superconductivity, it should be discussed by combining the structure analysis.

Superconductivity has been studied in various materials for a long time. Particularly, in recent years two-dimensional (2D) superconductivity at one or a few atomic layers has been reported[1–19] because of its interesting physical properties, e.g., anomalously large critical magnetic field in the in-plane direction,[1,2] significantly higher transition temperatures T_c at one-unit-cell layer compared to the bulk crystal,[3] and Berezinskii–Kosterlitz–Thouless transitions.[4–6] A straightforward way to discuss and understand such 2D superconducting properties is to compare the transport characteristics between bulk and thin films of the same materials.

Lead is a well-known superconducting material whose T_c and Bardeen–Cooper–Schrieffer coherence length at 0 K ξ_0 are 7.2 K[20] and 83 nm,[21] respectively, for three-dimensional (3D) bulk Pb. What happens to T_c and ξ_0 when the thickness of Pb decreases down to the atomic scale, i.e., the dimension changes from 3D to 2D? It has already been reported that 2D Pb structures show superconductivity and their T_c is suppressed owing to the reduced dimensionality.[2,5,11–18] For example, for Pb thin films grown on Si(111), T_c is dependent on the nominal film thickness,[2,5,11–13] and the value of the superconducting gap of Pb islands is affected by the geometric size of the islands.[13–15,19] Most of these studies have been performed using scanning tunneling spectroscopy (STS)[12–15,19] and have determined T_c locally from the superconducting energy gap. We need to observe the transition to zero resistance by transport measurement in order to discuss the superconducting properties at the macroscopic scale. However, there are only a few studies regarding the lateral transport properties along the surfaces of 2D Pb structures: in situ in vacuum[2] and ex situ in air.[5] On the other hand, to clarify the dimensionality of superconductivity, it is useful to compare ξ_0 with the film thickness.[9] The dependence of ξ_0 on film thickness is still unknown for thinner Pb films; only one paper by Ning et al. reports measurements of ξ_0 for Pb/Si(111) films with thickness of 25, 60, and 165 monolayer (ML)[21] by analyzing superconducting vortices by scanning tunneling microscopy (STM).

In this study, we investigated superconducting properties of Pb/Ge(111). The structure of Pb atomic layers grown at low temperature (LT) was measured by STM and reflection high-energy electron diffraction (RHEED). We measured the transport properties using an in situ four-point probe (4PP) method in ultrahigh vacuum (UHV) under a surface-normal magnetic field for two different structures: a continuous Pb film structure and a surface that is not fully covered by Pb islands. The former showed a superconducting transition similar to that of a Pb thin film on Si(111).[5,12,13] Surprisingly, the latter also showed zero resistance although Pb islands were not connected to each other, suggesting the presence of the proximity effect caused by the penetration of Cooper pairs from superconducting Pb islands to the wetting layer.

We obtained STM images by using the Omicron MULTIPROBE system in the constant-current mode with a mechanically cut PtIr tip after annealing in UHV. Transport measurements were performed using the in situ 4PP technique in a UHV system (Unisoku USM-1300S).[22] Since we used two separate UHV systems for STM and transport measurements, we paid close attention to determine the deposition amounts of Pb. The STM system is equipped with a hemispherical analyzer for angle-resolved photoemission spectroscopy; thus, we can confirm the Pb thickness by the energy band dispersion of quantum well states in the Pb film.[23–25] We can also determine the Pb deposition amount by RHEED oscillations for the transport measurement system.[25] The Pb coverages thus determined were cross checked by using various Pb-induced phases on a Si(111) substrate.[26] In both systems, we were able to determine the characteristics of the sample without exposing the surface to air.

An n-type Ge(111) substrate with a resistivity of 40–65 Ω cm at room temperature (RT), was cleaned by several cycles of 1.0 keV Ar^+ bombardment for 20 min and subsequent annealing up to 870 K for 20 min in UHV. We obtained a clean Ge(111)-c(2 × 8) surface structure on which Pb was deposited. It should be noted that the deposition temperature of Pb on the Ge substrate is very crucial for the growth of Pb atomic layers.[23,24,27–30] It has been reported that

when depositing Pb at RT, Ge(111)-β-$\sqrt{3}\times\sqrt{3}$-Pb superstructure is formed initially, and Pb(111) 1×1 islands are formed sparsely on the superstructure afterward.[28] On the other hand, other groups reported that the layer-by-layer growth of Pb layers on Ge(111) was realized by LT deposition.[23,24,30] In our study, therefore, Pb deposition was carried out on the Ge substrate at LT (~110 K) to obtain continuous atomic-layer structures. The Pb coverage was controlled by the deposition time at a constant deposition rate. The deposition rate was determined by using the formation of striped incommensurate (SIC) phase Pb/Si(111), which corresponds to 1.33 ML.[16,17,26,31] In our study, the definition of 1 ML is an atomic density of 7.22×10^{14} atoms/cm^2, equal to the atomic density of the Ge(111) unreconstructed surface.[27] We always maintained the substrate temperature below 110 K during Pb deposition and all processes in the chamber. We confirmed the 1×1 structure of Pb by RHEED pattern observation before and after transport measurement; therefore, it can be said the sample was maintained at low temperature during sample transfer in the chamber.

Figures 1(a)–1(e) show the RHEED patterns of Pb atomic layers on Ge(111) obtained at ~110 K for 0, 1, 3, 4, and 10 ML coverages, respectively. By the deposition of Pb, the fractional-order spots derived from the Ge(111)-c(2×8) reconstructed surface [Fig. 1(a)] became weaker, and then, they finally disappeared at 1 ML deposition, resulting in only Ge(111) 1×1 fundamental spots remaining [Fig. 1(b)]. With additional Pb deposition up to 3 ML [Fig. 1(c)], new streaks gradually came to appear at positions different from those of Ge(111) 1×1 fundamental spots which were simultaneously disappearing. At last, only those new streaks were observed with Pb coverage over 4 ML as shown in Figs. 1(d) and 1(e). The structural changes are more clearly expressed by the line profiles of the respective RHEED patterns in Fig. 1(f). By comparing to the known value of the lattice constant of Ge(111) (0.565 nm), we estimated the lattice constant of the 4 ML-Pb-deposited sample [Fig. 1(d)] to be 0.495 ± 0.007 nm. This value agrees well with that of Pb(111) 1×1 (0.492 nm), which implies that the Pb(111) thin film grows epitaxially on Ge(111) with Pb deposition more than 4 ML.

Next, STM measurements were performed on 0, 1, 3, and 10 ML coverages of Pb at ~110 K. Initially, the c(2×8) structure of Ge(111) clean surface was observed with atomic resolution [Fig. 2(a)]. After 1 ML deposition of Pb, the surface was not covered completely by small clusters of 2–3 nm in size [Figs. 2(b) and 2(e)], but the surface was fully covered by the wetting layer under clusters. The wetting layer showed a 4×4 periodicity only locally, while most of the areas of the wetting layer were not well-ordered. Thus, we could not discuss the structure and atomic density of the wetting layer, but the height of this layer was approximately one atomic layer of Pb.

At 3 ML coverage of Pb, Pb(111) 1×1 islands of around 10 nm in size were sparsely distributed as in Figs. 2(c) and 2(f), showing a Stranski–Krastanov-type (SK-type) structure. The 1×1 periodicity was observed on the Pb islands by atomic-resolution STM images, while no atomic images were obtained on the clusters. With 10 ML deposition of Pb, the surface was almost fully covered by Pb islands with different heights [Figs. 2(d) and 2(g)]. We can define it as a film

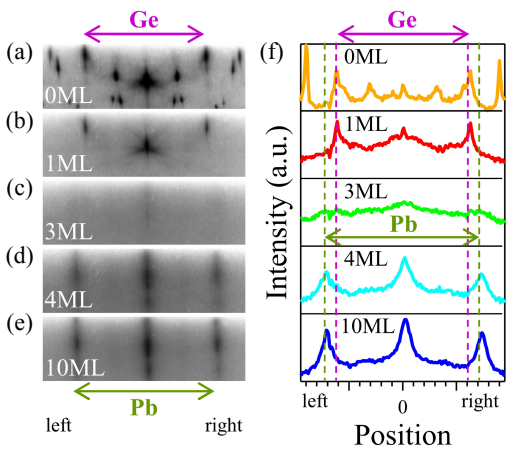

Fig. 1. (Color online) (a)–(e) RHEED patterns of Pb on Ge(111) deposited at ~100 K with different Pb coverages. (f) RHEED intensity profiles along a horizontal line near the shadow edge in (a)–(e). Purple and green dashed lines correspond to Ge(111) and Pb(111) lattice constants, respectively.

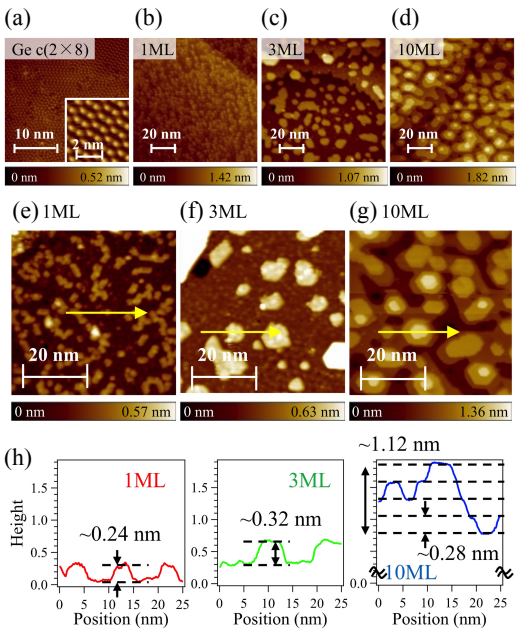

Fig. 2. (Color online) (a)–(g) STM images of Pb on Ge(111) with different Pb coverages. (a) Ge(111) c(2×8) clean surface ($V_b = +1.0$ V, $I_{set} = 1.0$ nA). (b, e) 1 ML-Pb ($V_b = +1.0$ V, $I_{set} = 0.2$ nA). (c, f) 3 ML-Pb [(c) $V_b = +1.0$ V, $I_{set} = 0.5$ nA, (f) $V_b = +0.2$ V, $I_{set} = 0.1$ nA]. (d, g) 10 ML-Pb ($V_b = +1.4$ V, $I_{set} = 0.1$ nA). (h) Line profiles along yellow arrows shown in (e)–(g).

exactly because of their atomic lattice periodicity and layer-by-layer growth. Hereafter, the SK-type structure at 3 ML and the film structure at 10 ML are collectively called 2D Pb structures.

Figure 2(h) shows the height profiles at different Pb coverages from Figs. 2(e), 2(f), and 2(g), respectively. One can see that the clusters and islands have different heights (0.24 nm measured from the wetting layer and 0.32 nm measured from clusters, respectively). The Pb island at 10 ML Pb coverage shows several steps (0.28 nm/step) which matches that of bulk Pb(111) lattice plane spacing (0.286 nm). The clusters can consist of not only deposited Pb atoms, but also Ge adatoms comprising the Ge(111)-c(2×8) reconstructed surface structure. However, these are not

distinguishable by STM. With Pb deposition more than 1 ML, more clusters appeared on the wetting layer, while the Pb islands appeared on the wetting layer for 3 ML-Pb deposition or more [Figs. 2(c) and 2(f)]. It seems that the height of Pb islands measured at 3 ML coverage is 0.32 nm above the clusters, which is different from the value of the Pb lattice plane spacing (0.286 nm) of bulk Pb(111) [Fig. 2(h)]. If Pb islands grow directly on the wetting layer, the total height from the wetting layer should be 0.56 nm = 0.24 nm (cluster) + 0.32 nm, which roughly corresponds to 2 ML Pb (= 0.286 × 2 nm). Below the Pb islands and clusters, the wetting layer exits. While its thickness is unknown, it should be around 1 ML. Then, the total amount of Pb including the wetting layer, clusters, and islands is more than 2 ML but less than 3 ML, which corresponds to the deposited amount. This estimation is reasonable when one considers the amount of Pb by the atomic density of Pb(111). We estimate the 3 ML-Pb/Ge sample in this study contains ~2.3 ML of Pb(111) because the definition of 1 ML is an atomic density of Ge(111), which corresponds to 0.766 ML of Pb(111) because of the different lattice constants between Ge(111) and Pb(111). The estimation of the thickness is also compatible with a sample of 10 ML Pb thickness.

Next, the transport results are discussed. We performed in situ 4PP transport measurements of these structures in UHV. The 4PP system consists of four copper wires of 100 μm in diameter, aligned on a line with a probe spacing of ~200 μm. The probes were gently brought in contact with the sample surface. The sample and probes were cooled down to ~0.8 K, and magnetic fields up to 7 T were applied perpendicular to the sample surface in UHV.

Figure 3(a) shows the temperature dependence of the sheet resistance of 1, 3, and 10 ML-Pb/Ge(111). We observed zero resistance for 3 and 10 ML-Pb, while 1 ML-Pb shows no sign of superconductivity down to 0.8 K. The resistance drop for 3 and 10 ML looks gradual even above T_c, which is typically observed in 2D superconductors.[1–3,5–11,17,18,25] Especially, the observation of the superconducting transition at 3 ML-Pb is remarkable because the surface is not entirely covered by Pb islands, as shown in Figs. 2(c) and 2(f).

First, we focus on the results of the 3 ML-Pb sample. The sheet resistance was measured as a function of temperature under different magnetic fields applied perpendicular to the sample surface [Fig. 3(b)]. We observed that superconductivity is broken under a magnetic field of 1.7 T. The magnetoresistance at different temperatures are also shown in Fig. 3(c). Here, the upper critical field [$\mu_0 H_{c2}(T)$] is extracted from Figs. 3(b) and 3(c), by defining $\mu_0 H_{c2}(T)$ at which the sheet resistance is half of the normal-state resistance. The obtained temperature dependence of $\mu_0 H_{c2}(T)$ is plotted in Fig. 3(d), which shows a linear relation with temperature. This is in the framework of the Ginzburg–Landau (GL) theory, as shown below:

$$\mu_0 H_{c2}^{\perp}(T) = \frac{\phi_0}{2\pi\xi_{GL}(0)^2}\left(1 - \frac{T}{T_c}\right), \tag{1}$$

where φ_0 is the flux quantum. From the fitting of the experimental data with Eq. (1), $\mu_0 H_{c2}(0)$ and the GL coherence length at 0 K [$\xi_{GL}(0)$] are estimated to be 1.5 T and 15 nm for 3 ML Pb coverage, respectively. There would be an argument that it is not reasonable to apply Eq. (1) to

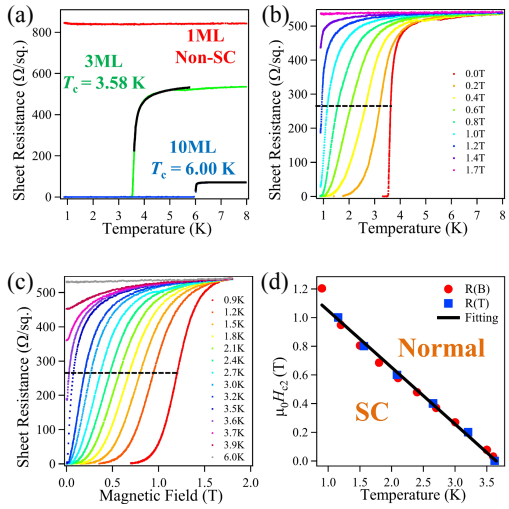

Fig. 3. (Color online) (a) Sheet resistance at 1, 3, and 10 ML Pb coverages as a function of temperature. $T_c = 3.58$ and 6.00 K for 3 and 10 ML, respectively, obtained by the theoretical fitting (black lines). (b, c) Sheet resistance of Pb 3 ML with temperature under different magnetic fields (b) and with magnetic field under different temperature (c). (d) Temperature dependence of the upper critical field obtained from (b) and (c). Solid black line denotes the fitting result by GL theory.

our 3 ML-Pb sample because it possesses an inhomogeneous structure as shown in Figs. 2(c) and 2(f). However, since we obtained the zero resistance globally, as the first attempt we apply the GL theory to our transport results assuming the 3 ML-Pb sample as a homogeneous 2D superconductor. Since this value of $\xi_{GL}(0) = 15$ nm is much longer than the film thickness (3 ML = 0.28 × 3 = 0.84 nm in average), we can conclude that the dimensionality of superconductivity is actually 2D. Thus it can be said that the gradual resistance drop above T_c in Fig. 3(a) is caused by the superconducting fluctuation of 2D superconductors.

We finally estimated T_c to be 3.58 K for 3 ML-Pb by fitting to the Aslamazov–Larkin–Maki–Thompson correction including the effect of the 2D superconducting fluctuation[32–34] as

$$\rho = \frac{1}{\sigma_0 + \sigma_{AL} + \sigma_{MT}}, \quad \sigma_{AL} = \frac{e^2}{16\hbar}\frac{T_c}{T - T_c},$$
$$\sigma_{MT} = \frac{e^2}{8\hbar}\frac{T_c}{T - (1+\delta)T_c}\ln\frac{T - T_c}{\delta T_c}, \tag{2}$$

where σ_0 and δ are the normal-state sheet conductivity and the pair-breaking parameter, respectively. The solid (black) lines fitted by Eq. (2) in Fig. 3(a) agree nicely with the experimental data.

Likewise, the sheet resistance of the 10 ML-Pb film was also measured while varying the magnetic field, as shown in Fig. 4(a). The critical magnetic field depends linearly on the temperature [Fig. 4(b)] again, similar to that as for the 3 ML-Pb sample. The fitting results are $\mu_0 H_{c2}(0) = 1.4$ T and $\xi_{GL}(0) = 15$ nm, which is still longer than the film thickness (0.286 × 10 = 2.86 nm on average). Thus, we conclude that the 10 ML-Pb film is also a 2D superconductor, for which we obtain a $T_c = 6.00$ K by the same theoretical fitting as for 3 ML-Pb [Fig. 3(a)].

Now, we discuss the origin of superconductivity in these 2D Pb structures. We illustrate the schematics of the structures in Fig. 4(c) for the respective Pb deposition

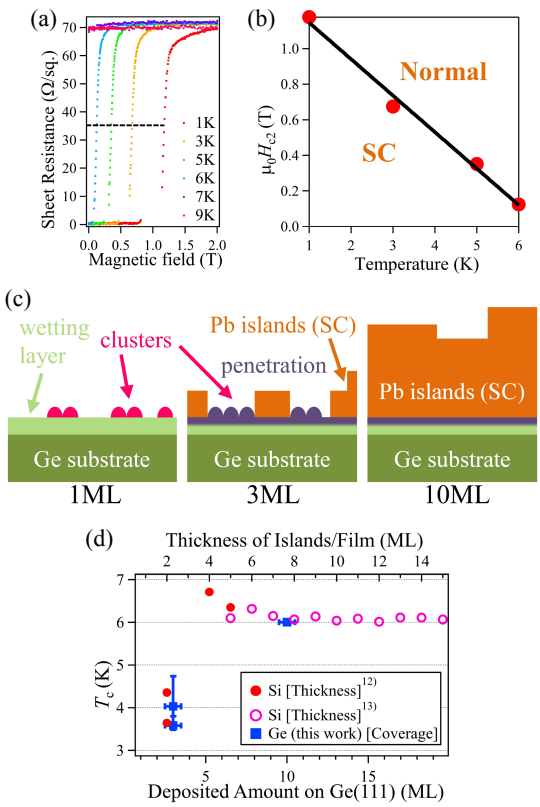

Fig. 4. (Color online) (a) Sheet resistance of 10 ML-Pb sample as a function of magnetic field under different temperatures. (b) Temperature dependence of the upper critical field obtained from (a). Solid black line is a fitting result by GL theory. (c) Schematics of 2D Pb structures, together with superconducting penetration areas caused by the proximity effect for 1 ML, 3 ML, and 10 ML-Pb samples. (d) The thickness/deposited amount dependence of T_c of 2D Pb structures on semiconductor substrates. Square dots (blue) indicate our result on Ge(111) using the bottom axis [1 ML is defined by the atomic density of Ge(111) unreconstructed surface]. Circle dots denote results on Si(111) in previous reports by Qin et al.[12] (filled, red) and Eom et al.[13] (open, pink), respectively, using the top axis [Thickness of islands/film measured from the wetting layer is defined by the atomic density of Pb(111)]. The deposition amounts are the same on the top and bottom axes.

amounts. The Pb film of 10 ML deposition shows superconductivity, where Pb(111) 1×1 islands cover the whole surface of the substrate. According to other 2D superconductors, the T_c of a thin film is lower than that of the bulk owing to the confinement effect.[2,11–18] Out result is consistent with those of the previous ones. In addition, the result for our 10 ML-Pb/Ge (~6 K) is in good agreement with that of 10 ML-Pb/Si (~6.1 K) in a previous report,[12] which implies the substrate does not affect the superconducting properties significantly.

In contrast, for the sample of 3 ML-Pb deposition, Pb islands are not interconnected [Figs. 2(c) and 2(f)]. A previous study of Pb islands on a β-$\sqrt{3} \times \sqrt{3}$-Pb/Ge(111) surface which was a different wetting layer structure from ours, reported the superconducting proximity effect by imaging the superconducting gap outside of a superconducting Pb island by STM.[28] They also reported that the length of the penetration of the superconducting gap feature extended by ~80 nm on the non-superconducting β-$\sqrt{3} \times \sqrt{3}$-Pb wetting layer at 0.5 K. If the penetration length in our sample was shorter than ~10 nm (average distance among Pb islands) below 3.6 K, the resistance should have shown a finite value below T_c because the superconducting areas are not connected to each other. This interpretation is reasonable, provided that the clusters on the 3 ML-Pb sample are non-superconducting as those on the 1 ML-Pb sample. This assumption is, however, reasonable by considering that T_c decreases below 3.6 K when the size of Pb islands becomes as small as a few nm according to Kim et al.[14] We also should consider the temperature dependence of the penetration length of the proximity effect. As is discussed by Cherkez et al.,[35] the penetration length tends to become shorter at higher temperature. Then, T_c by the proximity effect should be lower than the T_c of Pb islands. If so, the resistance reaches to zero by two-drops behavior in the temperature-resistance curve; the first drop at a high temperature is due to the superconducting Pb islands and the second drop (to zero resistance) at a lower temperature is due to the proximity effect. For our sample, however, we observed only a single resistance drop to zero at ~3.6 K as shown in Fig. 3. This means that the penetration length around 3.6 K in our 3 ML-Pb sample is long enough to connect the superconducting areas around Pb islands whose T_c is also around 3.6 K. At the T_c of Pb islands, the wavefunction of Cooper pairs spills out from superconducting Pb islands at a distance long enough to overlap each other and form superconducting paths throughout the whole surface.

Next, we discuss the reason for the lower T_c of 3 ML-Pb compared with that of 10 ML-Pb. As mentioned above, judging from the one-drop superconducting transition in Fig. 3, we can consider that the T_c ~3.6 K corresponds to the T_c of Pb islands themselves. Kim et al. reported that T_c of Pb islands on Si(111) tended to be lower as the islands become smaller.[14] In their experiments, the minimum size of the Pb islands was 15 nm and it showed a superconducting transition at ~4.4 K by STS measurement. Since, in general, T_c determined via transport measurements is lower than that via STS measurements due to the macroscopic nature of transport measurements,[17] it is reasonable that the T_c of Pb islands in 3 ML-Pb/Ge is even lower because our Pb islands are smaller than 15 nm and T_c is determined by transport measurements.

We are convinced that the origin of the superconducting transition of 3 ML-Pb/Ge(111) is different from that of the 10 ML-Pb sample. We summarize our results in Fig. 4(d) by plotting the T_c as a function of the deposited amount of Pb (see bottom axis) and combining our data with previous data on Pb/Si(111) by Qin et al.[12] and Eom et al.[13] (see top axis). The top axis and bottom axis correspond to each other to indicate the sample amounts of deposition. For our 10 ML-Pb sample, the T_c is very similar (~6 K) among the reports, irrespective of the substrates. By taking the results of the STM measurement into account, we suggest that the 10 ML-Pb film grows layer-by-layer above some critical thickness on both Si and Ge. This indicates that the film is little affected by the substrate above a certain thickness of the Pb. The comparatively lower T_c compared to bulk Pb can be explained by the limited dimensionality in both the Si and Ge cases, as shown in Fig. 4(d). When we focus on T_c only, there is almost no difference between Si(111) and Ge(111) substrates above 8 ML Pb deposition.

However, at thinner Pb 2D structures, the structures of the wetting layer and islands/clusters are not the same on the two substrates. As mentioned above, the inhomogeneous struc-

tures of 3 ML-Pb/Ge(111) surface shows superconductivity owing to the proximity effect. On the other hand, when Pb(111) thin films are grown epitaxially on Si(111) above thicknesses of 2 ML, the superconductivity is not induced by the proximity effect, but rather by the direct coalescence of superconducting Pb islands. Therefore, the origin of superconductivity at lower thickness may be different even if T_c has similar values on the two substrates. When one discusses what induces superconductivity in a 2D system, it is very important to combine structure analysis at the microscopic scale with transport properties. Moreover, since the superconducting proximity effect has been recently frequently used to make topological superconductors, it would be important to correlate the structures and the property of the spill out of the Cooper pair wavefunction in the non-superconducting phases.[36–38]

Finally, we discuss the 1 ML-Pb sample, which has only small clusters on the wetting layer. We could not observe superconductivity on the 1 ML-Pb sample. It means that the wetting layer is not superconducting by itself. When clusters are not connected to each other, we would have observed a small resistance drop to a finite value at ~3.6 K if the clusters themselves were superconductors. However, we observed no such resistance drop at the 1 ML sample. Therefore, it is suggested that Pb clusters do not show superconducting transition. Therefore, the superconductivity at our 3 ML-Pb sample is not thought to be caused by the clusters themselves on the wetting layer. In other words, the 3 ML-Pb sample needs Pb(111) islands to show superconductivity.

In conclusion, we studied the superconducting properties of Pb atomic layers grown on the Ge(111) surface. By depositing Pb at 110 K, Pb atoms formed tiny clusters and larger Pb(111) islands on the wetting layer. By further increasing the Pb coverage, the Pb(111) islands coalesce to make a continuous thin film. As the result of the in situ 4PP transport measurements, a superconducting transition was observed for 3 and 10 ML coverages around 4 and 6 K, respectively, showing the nature of 2D superconductors. The 2D superconductivity at 3 ML is interpreted to be induced by the proximity effect in which the wavefunction of Cooper pairs spills out from the unconnected superconducting Pb(111) islands. We suggest that the understanding of structure in microscopic scale is crucial to reveal superconductivity in atomic-layer 2D systems.

Acknowledgment We thank R. Akiyama and R. Hobara for their useful discussion and assistance in the experiments. This work was supported by the JSPS (KAKENHI 16H02108 and Bilateral Joint Research Project with RFBR) and Russian Foundation for Basic Research (Grant 18-52-50022).

*h.toyama@surface.phys.s.u-tokyo.ac.jp

1) Y. Saito, Y. Kasahara, J. Ye, Y. Iwasa, and T. Nojima, Science **350**, 409 (2015).
2) T. Sekihara, R. Masutomi, and T. Okamoto, Phys. Rev. Lett. **111**, 057005 (2013).
3) S. He, J. He, W. Zhang, L. Zhao, D. Liu, X. Liu, D. Mou, Y.-B. Ou, Q.-Y. Wang, Z. Li, L. Wang, Y. Peng, Y. Liu, C. Chen, L. Yu, G. Liu, X. Dong, J. Zhang, C. Chen, Z. Xu, X. Chen, X. Ma, Q. Xue, and X. J. Zhou, Nat. Mater. **12**, 605 (2013).
4) S. Ichinokura, L. V. Bondarenko, A. Y. Tupchaya, D. V. Gruznev, A. V. Zotov, A. A. Saranin, and S. Hasegawa, 2D Mater. **4**, 025020 (2017).
5) W. Zhao, Q. Wang, M. Liu, W. Zhang, Y. Wang, M. Chen, Y. Guo, K. Hea, X. Chen, Y. Wang, J. Wang, X. Xie, Q. Niu, L. Wang, X. Ma, J. K. Jain, M. H. W. Chan, and Q.-K. Xue, Solid State Commun. **165**, 59 (2013).
6) A. V. Matetskiy, S. Ichinokura, L. V. Bondarenko, A. Y. Tupchaya, D. V. Gruznev, A. V. Zotov, A. A. Saranin, R. Hobara, A. Takayama, and S. Hasegawa, Phys. Rev. Lett. **115**, 147003 (2015).
7) N. Reyren, S. Thiel, A. D. Caviglia, L. F. Kourkoutis, G. Hammerl, C. Richter, C. W. Schneider, T. Kopp, A.-S. Rüetschi, D. Jaccard, M. Gabay, D. A. Muller, J.-M. Triscone, and J. Mannhart, Science **317**, 1196 (2007).
8) J. T. Ye, S. Inoue, K. Kobayashi, Y. Kasahara, H. T. Yuan, H. Shimotani, and Y. Iwasa, Nat. Mater. **9**, 125 (2010).
9) T. Uchihashi, Supercond. Sci. Technol. **30**, 013002 (2017).
10) T. Uchihashi, P. Mishra, M. Aono, and T. Nakayama, Phys. Rev. Lett. **107**, 207001 (2011).
11) Y. Guo, Y.-F. Zhang, X.-Y. Bao, T.-Z. Han, Z. Tang, L.-X. Zhang, W.-G. Zhu, E. G. Wang, Q. Niu, Z. Q. Qiu, J.-F. Jia, Z.-X. Zhao, and Q.-K. Xue, Science **306**, 1915 (2004).
12) S. Qin, J. Kim, Q. Niu, and C.-K. Shih, Science **324**, 1314 (2009).
13) D. Eom, S. Qin, M.-Y. Chou, and C. K. Shih, Phys. Rev. Lett. **96**, 027005 (2006).
14) J. Kim, G. A. Fiete, H. Nam, A. H. MacDonald, and C.-K. Shih, Phys. Rev. B **84**, 014517 (2011).
15) J. Liu, X. Wu, F. Ming, K. Wang, and X. Xiao, Supercond. Sci. Technol. **26**, 085009 (2013).
16) T. Zhang, P. Cheng, W.-J. Li, Y.-J. Sun, G. Wang, X.-G. Zhu, K. He, L. Wang, X. Ma, X. Chen, Y. Wang, Y. Liu, H.-Q. Lin, J.-F. Jia, and Q.-K. Xue, Nat. Phys. **6**, 104 (2010).
17) M. Yamada, T. Hirahara, and S. Hasegawa, Phys. Rev. Lett. **110**, 237001 (2013).
18) Y. Liu, Z. Wang, X. Zhang, C. Liu, Y. Liu, Z. Zhou, J. Wang, Q. Wang, Y. Liu, C. Xi, M. Tian, H. Liu, J. Feng, X. C. Xie, and J. Wang, Phys. Rev. X **8**, 021002 (2018).
19) T. Nishio, M. Ono, T. Eguchi, H. Sakata, and Y. Hasegawa, Appl. Phys. Lett. **88**, 113115 (2006).
20) B. Mitrović, H. G. Zarate, and J. P. Carbotte, Phys. Rev. B **29**, 184 (1984).
21) Y.-X. Ning, C.-L. Song, Y.-L. Wang, X. Chen, J.-F. Jia, Q.-K. Xue, and X.-C. Ma, J. Phys.: Condens. Matter **22**, 065701 (2010).
22) M. Yamada, T. Hirahara, R. Hobara, S. Hasegawa, H. Mizuno, Y. Miyatake, and T. Nagamura, e-J. Surf. Sci. Nanotechnol. **10**, 400 (2012).
23) S.-J. Tang, C.-Y. Lee, C.-C. Huang, T.-R. Chang, C.-M. Cheng, K.-D. Tsuei, and H.-T. Jeng, Appl. Phys. Lett. **96**, 103106 (2010).
24) R.-Y. Liu, A. Huang, C.-C. Huang, C.-Y. Lee, C.-H. Lin, C.-M. Cheng, K.-D. Tsuei, H.-T. Jeng, I. Matsuda, and S.-J. Tang, Phys. Rev. B **92**, 115415 (2015).
25) H. Toyama, H. R. Huang, T. Nakamura, L. V. Bondarenko, A. Y. Tupchaya, D. V. Gruznev, A. Takayama, A. V. Zotov, A. A. Saranin, and S. Hasegawa, Defect Diffus. Forum **386**, 80 (2018).
26) K. Horikoshi, X. Tong, T. Nagao, and S. Hasegawa, Phys. Rev. B **60**, 13287 (1999).
27) L. Seehofer, G. Falkenberg, D. Daboul, and R. L. Johnson, Phys. Rev. B **51**, 13503 (1995).
28) H. Kim, Y. Miyata, and Y. Hasegawa, Supercond. Sci. Technol. **29**, 084006 (2016).
29) K. Yaji, Y. Ohtsubo, S. Hatta, H. Okuyama, K. Miyamoto, T. Okuda, A. Kimura, H. Namatame, M. Taniguchi, and T. Aruga, Nat. Commun. **1**, 17 (2010).
30) L. Grill, D. Cvetko, L. Petaccia, F. Ratto, and S. Modesti, Surf. Sci. **562**, 7 (2004).
31) W. B. Jian, W. B. Su, C. S. Chang, and T. T. Tsong, Phys. Rev. Lett. **90**, 196603 (2003).
32) R. S. Thompson, Phys. Rev. B **1**, 327 (1970).
33) A. Larkin and A. Varlamov, *Theory of Fluctuations in Superconductors* (Clarendon Press, Oxford, U.K., 2005).
34) K. Maki, Prog. Theor. Phys. **39**, 897 (1968).
35) V. Cherkez, J. C. Cuevas, C. Brun, T. Cren, G. Ménard, F. Debontridder, V. S. Stolyarov, and D. Roditchev, Phys. Rev. X **4**, 011033 (2014).
36) J.-P. Xu, M.-X. Wang, Z. L. Liu, J.-F. Ge, X. Yang, C. Liu, Z. A. Xu, D. Guan, C. L. Gao, D. Qian, Y. Liu, Q.-H. Wang, F.-C. Zhang, Q.-K. Xue, and J.-F. Jia, Phys. Rev. Lett. **114**, 017001 (2015).
37) H.-H. Sun and J.-F. Jia, npj Quantum Mater. **2**, 34 (2017).
38) T. Uchihashi, Nanotechnology **26**, 344004 (2015).

